INDIAN SPACE RESEARCH ORGANISATION

# Retrieval and Validation of Pressure Fields from Scatterometer Winds

**Version 1.0**

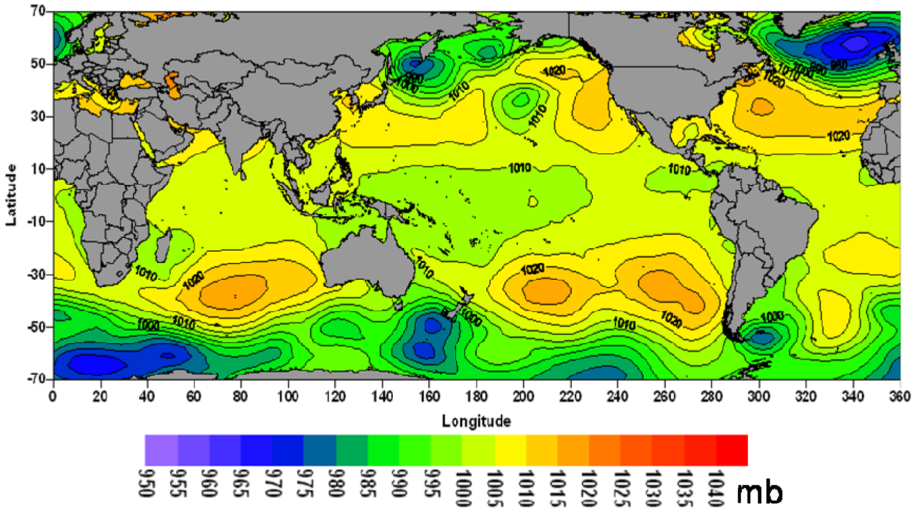


**Ocean Sciences Group**
**Earth and Climate Science Area**
**National Remote Sensing Centre**
**Hyderabad, India**

nrsc

**June, 2015**

**NATIONAL REMOTE SENSING CENTRE**

**REPORT / DOCUMENT CONTROL SHEET**

| | | | | | |
|---|---|---|---|---|---|
| **1.** | **Security Classification** | Unclassified | | | |
| **2.** | **Distribution** | Through soft and hard copies | | | |
| **3.** | **Report / Document version** | **(a) Issue no.:**01 | **(b) Revision & Date:** R02/November 2014 | | |
| **4.** | **Report / Document Type** | Technical Report | | | |
| **5.** | **Document Control Number** | **NRSC – ECSA – OSG – NOV – 2014 – TR – 667** | | | |
| **6.** | **Title** | **Retrieval and Validation of Pressure Fields from Scatterometer Winds** | | | |
| **7.** | **Particulars of collation** | **Pages:** 27 | **Figures: 17** | **References:** 26 | |
| **8.** | **Author (s)** | Ch Purnachand, I V Ramana, M M Ali, K H Rao, P N Sridhar, C B S Dutt and M V Rao | | | |
| **9.** | **Affiliation of authors** | Ocean Sciences Group, ECSA, NRSC, Hyderabad; | | | |
| **10.** | **Scrutiny mechanism** | **Prepared by** M V Rao, OSG (ECSA) | **Compiled by** P N Sridhar OSG (ECSA) | **Reviewed by** GD (OSG) | **Approved** DD (ECSA) |
| **11.** | **Originating unit** | Ocean Sciences Group, ECSA, NRSC | | | |
| **12.** | **Sponsor (s) / Name and Address** | NRSC, Balanagar, Hyderabad | | | |
| **13.** | **Date of Initiation** | November, 2014 | | | |
| **14.** | **Date of Publication** | June, 2015 | | | |
| **15.** | **Abstract:** The pressure charts prepared by interpolating point measurements/generated through Numerical Weather Forecast (NWF) models or data assimilation techniques. But these data sets may not provide true field situation. As of today, no remote sensing sensor is capable to measure the pressure fields directly. In the present technical report we presented the methodology of retrieve pressure fields from Quick-Scat/Oceansat-2 Scatterometer (OSCAT) winds using the University of Washington Planetary Boundary Layer (UWPBL) model of Patoux et al (2003) during some selected period. These pressure values are validated with all the available in situ observations and the results are presented. **Key Words:** *Oceansat-2, Scatterometer, Winds, Pressure fields, DIVA and UWPBL model.* | | | | |

## Contents

## 1.0 Introduction:

Surface pressure fields are generally obtained by contouring measurements of surface pressure observation from in-situ observations like weather stations, Radio sonders, Buoy/Ships or numerical Model or data assimilation system. The Mean Sea Level Pressure Analysis is one of the most familiar images in the community seen daily on television, in some newspapers, and on the web, these images are compiled from hundreds of weather observations (synoptic data) taken simultaneously around the world. The mean sea level pressure charts so compiled show weather systems like highs, lows including tropical cyclones. These charts also indicate how the weather patterns are expected to develop. Everyone benefits from a better understanding of the Mean Sea Level Pressure (MSLP) analysis and prognostic charts, especially people whose activities are particularly weather-sensitive such as pilots, farmers, mariners, builders: who often find the maps or charts valuable, sometimes essential, to enhance their understanding of media forecasts and help from their own ideas based on local experience.

Sea level varies from day to day and week to week, depending on the weather situation. Air pressure has a direct influence on the sea level. High air pressure exerts a force on the surroundings and results in water movement. So high air pressure over a sea area corresponds to low lea level and conversely low air pressure (depression) results in higher sea levels. This leads to ocean circulation. While trying to forecast year to year fluctuations in Indian summer monsoon, Sir Gilbert Walker shown that large scale atmospheric oscillations over the southern hemisphere exists and he had termed it as Southern Oscillation (SO). Hence the information on MSLP provide a unique opportunity to examine the circulation patterns associated with extreme events across the oceans, such as heat wave, El-Nino and southern oscillation (ENSO) in the context of historical events. Atmospheric General Circulation Models (AGCM) has considerable skill in reproducing the observed seasonal reversal of MSLP, the location of the summer heat low as well as the position of the monsoon trough over the Indian subcontinent, the present-day climate and its seasonal cycle are realistically simulated by the model over this region.

The ability to obtain surface pressure fields from Scatterometer data has been demonstrated by Brown and Levy 1986; Harlan and O'Brien 1986; Hsu et al. 1997; Hsu and Liu 1996; Zieren et al. 2000, and the value of the surface pressure fields product from satellite scatterometers has been shown in several applications. Firstly Levy & Brown 1991 and Brown &Zeng 1994 have shown shortcomings in the wind vectors of numerical analyses using Seasat and the first European Remote Sensing Satellite (ERS-I) winds in the tropics and southern hemisphere. Using surface pressure gradients from buoy data as surface truth for scatterometer winds derived pressure gradients, impetus was furnished to change the scatterometer model function and "climatology" to increase winds in the moderate range and add very high winds in storms (Fster and Brown 1994; Brown 1998,2000; Zeng and Brown 1998,2001). The use of the surface pressure fields as a smoothing product allowed Patoux and Brown (2001 & 2002) to produce continuous Sea Winds-on-QuikScatterometer (QSCAT) wind fields in the midlatitudes. However, these methods have been inherently limited to the midlatitudes and do not resolve the pressure distribution near the equator. For many years, this has been a hurdle in using scatterometer data for computing swath-long (i.e, pole to pole) surface pressure fields.

General circulation models with mesoscale resolution will benefit from assimilation the Scatterometer winds (Conaty et al. 2001), as well as from the meso-scale structure present in the corresponding surface pressure fields. A scheme that estimates the surface pressure in the tropics as well as in the mid - latitudes would thus provide two quasi-global marine surface pressure fields per day. Moreover, a systematic estimation of surface pressure from scatterometer winds over the tropical ocean would be an improvement over the sparse pressure observations from isolated buoys, islands, and ships.

Stevens et al. (2002) (STN) described a simple mixed- layer model for the tropical planetary boundary layer (PBL) based on a force balance among pressure gradient force, Coriolis force, surface drag, and entrainment flux of free-tropospheric momentum into the boundary layer. They apply it to a climatological dataset of surface pressures and free-trpospheric surface winds, by matching the estimated surface winds to the climatological values they derived two optimal parameters for the inclusion of entrainment into the PBL structure. These are the entrainment rate and the boundary layer depth, which are assumed to have constant values over the domain, the resulting model is successful in reproducing the climatolgical surface winds fields. Patoux et al. 2003 applied the inverse of this model to estimate pressure gradients (subsequently the surface pressure the ability to obtain surface pressure fields from scatterometer starting from Seasat-A Space-borne Scatterometer (SASS) data has been demonstrated. From the surface wind fields in the tropics and then blended this PBL model with the midlatitude model to provide a continuous global model.

## 2.0 The University of Washington Planetary Boundary Layer (UWPBL) model:

Retrieval of pressure fields from Ocean Sat - II Scatterometer (OSACT) winds utilized Patoux et al., (2003) UWPBL method. The retrieval of a pole-to-pole oceanic surface pressure field is a four-step process: surface pressure gradients are obtained in the mid-latitudes with a two-layer similarity PBL model; they are obtained in the Tropics with a mixed-layer model; three pressure fields (Northern Hemisphere, Tropics, Southern Hemisphere) are obtained from the pressure gradient fields by least squares optimization; and the three pressure fields are blended in the overlapping latitudinal bands. The resulting pressure pattern is given an absolute value using one or more pressure observations.

By definition, in the midlatitudes, the “direct" model calculates the surface wind from knowledge of the geostrophic wind. The “inverse" model calculates the geostrophic wind at the top of the boundary layer from values of the surface wind. They include parameterizations for stratification, thermal wind and secondary flows. In the Tropics, the “mixed layer model" calculates the pressure gradient at the top of the boundary layer from values of the surface wind and free tropospheric wind. By extension, “inverse model" also refers to the “pressure retrieval model", which calculates the surface pressure gradient at each point of a horizontal grid and it’s a pressure pattern to the resulting vector field.

### 2.1 Two - layer similarity model

The University of Washington Planetary Boundary Layer (UWPBL) model used to calculate gradient or geostrophic wind vectors from surface wind vectors (the so-called inverse model) has been extensively documented (Brown and Levy 1986; Brown and Liu 1982; Brown and Zeng 1994; Patoux 2000). Because the new element here is the mixed-layer model in the Tropics, the mid-latitude solution will be only briefly described. In the midlatitudes, the wind profile in the boundary layer is resolved by patching a modified Ekman spiral (outer layer) to a logarithmic profile (inner layer). The matching conditions at the patch height between the Ekman layer and the so-called “log"-layer (or surface layer, or constant-flux layer) yield simple similarity relations between the surface stress and the geostrophic flow (Brown, 1982). Stratification, baroclinicity and secondary flows can be taken into account. At each point of a scatterometer swath or numerical model grid for which a surface wind vector is available, the PBL wind profile is approximated by patching a modified Ekman spiral to a logarithmic surface layer. Stratification and baroclinicity (Foster et al. 1999; Foster and Levy 1998) are taken into account by including surface air temperature, sea surface temperature, and relative humidity, where available (typically, gridded fields from an NWF analysis). Secondary flows are parameterized (Brown 1970, 1981). The gradient wind vector is thus estimated and the corresponding geostrophic wind vector and pressure gradient are calculated using the gradient wind correction described in Patoux and Brown (2002)

### 2.2 Mixed - layer model

As we approach the equator, the Coriolis force decreases and the midlatitude model fails to approximate the boundary layer dynamics correctly, primarily due to its assumption of Ekman layer dynamics and lack of entrainment processes. The Ekman depth becomes infinite and the modified Ekman spiral model is not valid. We use instead the simple model described in Patoux et al. (2003) and based on the mixed layer model by Stevens et al. (2002).

A first guess is made on the pressure gradient, assumed constant throughout the boundary layer, and a first wind profile is obtained. The bulk wind is calculated by integration of this profile and a new estimate of the pressure gradient is obtained from the bulk force balance. A final value for the pressure gradient is obtained by convergence within a few iterations. From a swath of scatterometer surface winds, a field of pressure gradients can be calculated and used as an input to the pressure retrieval model.

The model computes pressure fields in four steps. Solving the following equations to obtain wind profile with boundary condition at the surface (scatterometer wind) and at the top climatological free topospheric wind from a classical fourth-order Runge-Kutta Method (Press et al 1992)

$$\frac{d}{dz}\left(K\frac{d\bar{u}}{dz}\right) = \frac{1}{\rho_o}\left(\frac{\partial p}{\partial x}\right) - f\,\bar{v},$$

$$\frac{d}{dz}\left(K\frac{d\bar{v}}{dz}\right) = \frac{1}{\rho_o}\left(\frac{\partial p}{\partial y}\right) - f\,\bar{u}, \quad and$$

$$K = \frac{k u_* h}{\Phi_m(\zeta)}\left[\frac{z}{h}\left(1 - \frac{z}{h}\right)^2\right]$$

Calculate bulk wind by integrating the profile obtained in step 1 and estimate new pressure gradient using the following equations

$$\frac{P_x}{\rho} = f\,V - \frac{w_e}{h}\left(U_\tau - U\right) + \frac{u_*^2}{h}\frac{u_{10}}{|u_{10}|} \quad and$$

$$\frac{P_y}{\rho} = f\,U - \frac{w_e}{h}\left(V_\tau - V\right) + \frac{u_*^2}{h}\frac{v_{10}}{|u_{10}|}$$

Iterate step 1 and step 2 till convergence to get final value of pressure gradient

Retrieve zero mean pressure values from pressure gradients using the following equations

$$\mathbf{H} = \begin{vmatrix} \dfrac{1}{a\cos\Phi}\dfrac{\partial}{\partial\lambda} \\ \dfrac{1}{a}\dfrac{\partial}{\partial\Phi}, \end{vmatrix} \qquad \mathbf{x} \equiv \mathbf{P}, \text{ and } \quad \mathbf{y} \equiv \begin{vmatrix} \mathbf{P}_{\lambda} \\ \mathbf{P}_{\Phi}, \end{vmatrix}$$

$$\left| \mathbf{H^T H x} - \mathbf{H^T y} \right|^2 \equiv 0$$

Finally obtain values of pressure (y) using least square fit from buoy measurements

$$\mathbf{Hx = y}$$

The Steps involved are presented in following flow diagram

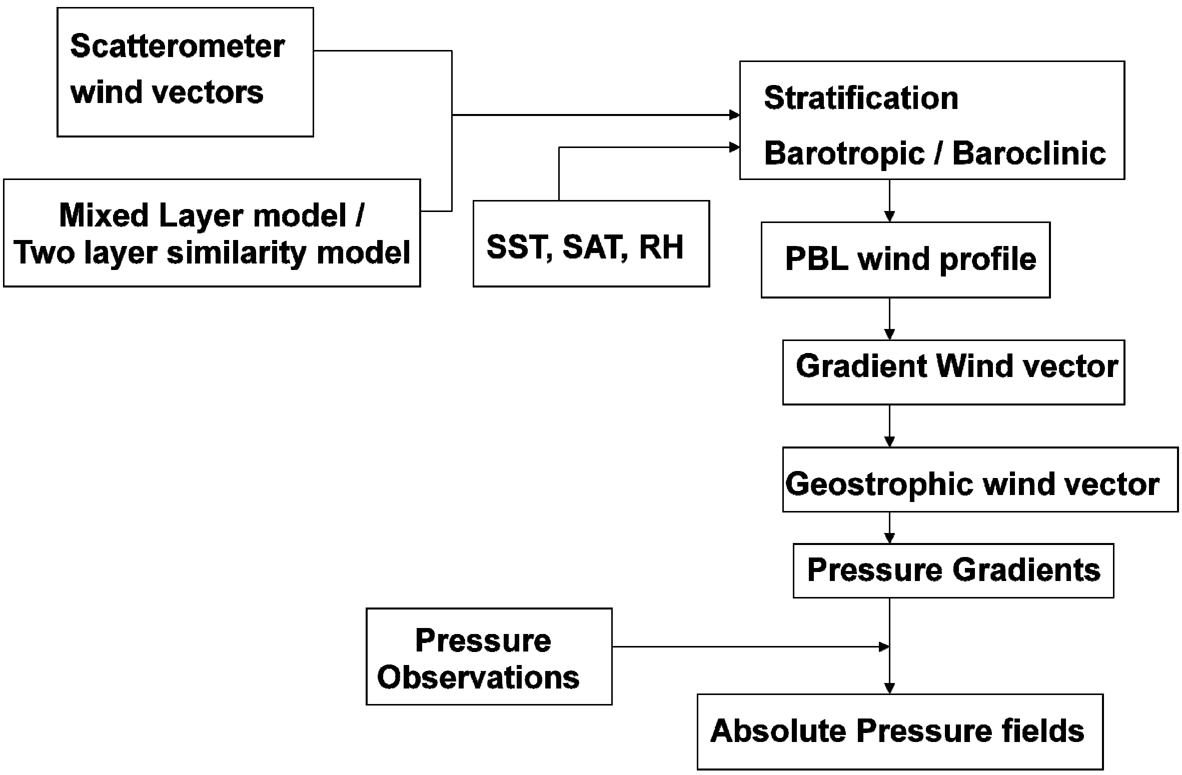


Figure 1. Flow diagram depicting the process steps in the retrieval of pressure fields using UWPBL model from Scatterometer winds.

### 2.3 Initial pressure values or pressure observations:

When integrating from pressure gradients to pressure, the constant of integration can be set to be either a standard pressure value or an in-situ pressure measurement at the time of scatterometer observations or all available in situ observations as first guess pressure value.

## 3.0 Oceansat-2 Scatterometer (OSCAT):

OSCAT is onboard the Indian Oceansat-2 satellite along with two other sensors, an ocean color monitoring sensor and a radio occultation sounder for the atmosphere. OSCAT is a Ku band pencil beam scatterometer similar to the NASA Sea Winds-on-QuikSCAT scatterometer.

The Ku-band pencil beam scatterometer is active microwave radar operating at 13.515 Ghz, It consists of a parabolic 1m diameter dish antenna rotating at 20 revolutions per minute (rpm) using a DC motor and generates two beams. The inner beam operates with HH polarization while the outer beam operates with VV polarization. The scatterometer covers a swath of 1800km in width. The energy of the transmitted RF pulse backscattered by the ocean surface is received at the antenna and, after on-board 'range compression', is digitized and transmitted to the ground station. The normalized radar cross section, referred to as Sigma-naught ($\sigma_o$), is calculated from this echo and the wind vector is derived using a Geophysical Model Function before being provided to the users in 50 km X 50km cell size. The derived wind speed ranges from 4-24 m $s^{-1}$ with an accuracy of better than 20% (rms) for the wind magnitude and direction.

## 4.0 Data Used:

In this present study utilized OSCAT Level 2B wind data from NRSC, ISRO, and QSCAT Level 2B from Physical Oceanography Distributed Active Archive Center (PO.DAAC). The in-situ pressure observations are taken from Indian National Centre for Ocean Information Services (INCOIS), India Meteorological Department & Global Telecommunication System (GTS).

The OSCAT 50 km x 50 km resolution wind data is given as input and generated output in grid size of $0.5^0$ x $0.5^0$ gridded data along path pressure field during January - February 2010, 2011 and 2012 over North Indian Ocean (NIO). The OSCAT data processed for the retrieval of pressure fields during recent cyclones viz; Jal - November, 2010, Nilam - Oct-Nov 2012, Mahasen - May 2013, Phailin - October, 2013, Lehar – November, 2013 and Madi - December, 2013. The salient results are presented. All the 14 passes of OSCAT in a day are processed to retrieve the global pressure fields as a single daily product. These products are validated using buoy pressures obtained through GTS.

# 5.0 Retrieval of pressure fields during Very Severe Cyclonic Storms:

## 5.1 Jal

Severe Cyclonic Storm Jal is the fifth named cyclonic storm and the fourth Severe Cyclonic Storm of the 2010 North Indian Ocean cyclone season. Jal developed from a low pressure area in the South China Sea that organized into a Tropical Depression on October 28. At least 54 people are known to have been killed in India. Early on November 6, the IMD upgraded Depression BOB 05 to a deep depression. Later, the deep depression strengthened further, prompting the IMD to upgrade it to a cyclonic storm, and was named "Jal". The storm continued to grow and became a severe cyclonic storm by November 6. On November 7, Jal started weakened. Soon afterward, the IMD reported that Jal weakened into a Cyclonic Storm. Late on the same day, the IMD reported that the storm weakened into a Deep Depression. As a deep depression, the system made landfall at Chennai, a few hours later.

The pressure fields are retrieved during JAL cyclone in November 7$^{th}$, 2010 using Oceansat-II Scatterometer wind and the results are presented in figure 2. The pressure retrievals are compared with those of pressure maps provided by Bureau of Meteorology, Govt. of Australia for Jal cyclone and the patterns are comparable.

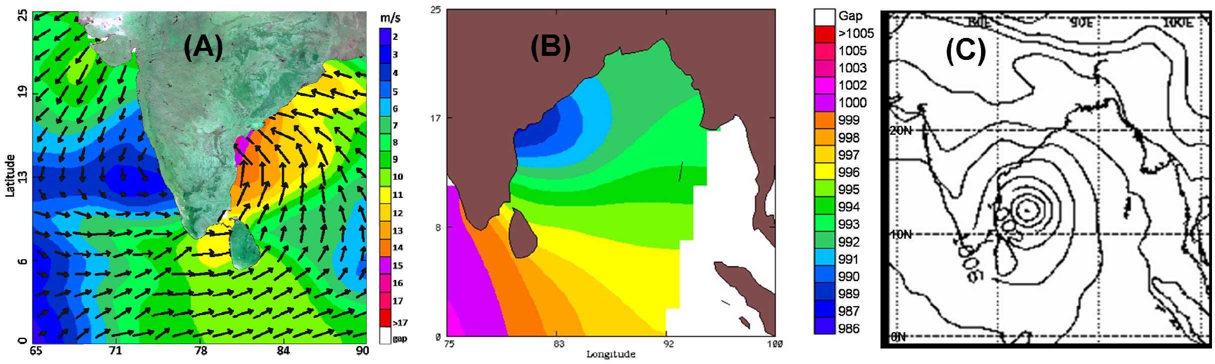


Figure 2. (a) Scatterometer wind vectors of OSCAT, during November 7, 2010 (b) OSCAT scatterometer derived pressure fields during Jal cyclone on during November 7, 2010 and (c) MSL pressure maps provided by Bureau of Meteorology, Govt. of Australia during this period.

## 5.2 Nilam

A well marked low pressure that had developed in the early hours of October 27, 2012 over south central Bay of Bengal and was intensified into a Cyclonic Storm in the morning of 30th October off Sri Lanka coast and named it as Nilam. The Cyclonic Storm, Nilam then moved north-northwest-wards, crossed north Tamilnadu coast near Mahabalipuram, south of Chennai between 1600 and 1700 hrs IST of 31st October 2012. Under its influence gale wind speed reaching 70-80 kmph prevailed along and off north coastal Tamil Nadu, Puducherry and adjoining south Andhra Pradesh coast. As a consequence of this cyclone, a total of 75 lives lost along with devastation of habitations and agriculture to the tune of few hundred crore rupees due to heavy to very heavy rainfall as well as gale winds.

The pressure fields are calculated from the L2B Oceansat-2 Scatterometer (OSCAT) surface wind vectors during the continuous coverage of Nilam cyclone area (27 October to 02 November 2012) over Bay of Bengal using UWPBL Model of Patoux et al (2003). To estimate actual pressure values from pressure gradients, we used different constants of integration in our analysis as first guess value, based on the available moored buoy observations in the Bay of Bengal. The pressure fields estimated during 28 October2012 to 31 October 2012 by inputting all the individual pressure values as first guess value and are presented in Fig. 3. The scatterometer-derived sea-level pressure fields describe the movement and intensity of the cyclone well.

The retrieved pressure fields were compared buoy observations. Best results are obtained when individual pressure values from all the buoys are taken into account instead of a constant or average of buoy observations, with a RMSD of $\pm$ 0.67 and a bios of -0.06. Very poor results were obtained when a constant pressure of 1013 hPa is used. The details of study carried during Nilam cyclone are presented in Purna chand et al (2013).

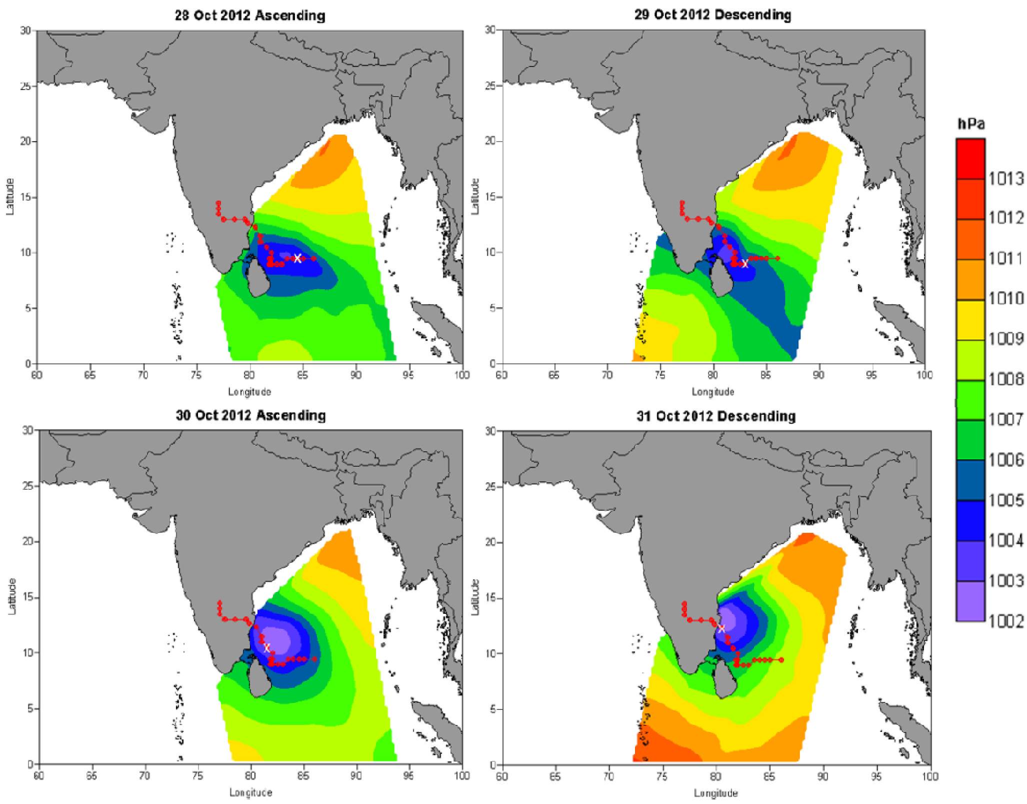


Figure - 3: After Purnachand et al (2013), Distribution of sea level pressure along with cyclone Tracks. The centre of the cyclone location is marked as "X" on the figures.

## 5.3 Mahasen

In early May 2013, an area of low pressure over the southern Bay of Bengal was originated and was slowly consolidated into a depression on May 10. The depression gained forward momentum and attained gale-force winds on May 11 and was designated as Cyclonic Storm “Mahasen”, Early on May 16, the cyclone attained its peak intensity with winds of 85 km/h (50 mph) and a barometric pressure of 990 mbar. Shortly thereafter Mahasen made landfall near Chittagong, Bangladesh. On May 17, it moved over the eastern Indian state of Nagaland. Cyclonic Storm Mahasen was a relatively weak tropical cyclone that caused loss of life and property across six countries in Southern and Southeastern Asia.

A complimentary study has been carried out to the retrieval of Sea Level Pressure fields from OSCAT wind field data of Mahasen Cyclone (May 10 to May 16, 2013) using University of Washington Planetary Boundary Layer (UWPBL) model of Patoux et al (2003). The information on cyclone track and intensity was obtained from the India Meteorological Department (IMD). The strengthening of Deep Depression during 10$^{th}$ may 2013 into severe cyclonic storm by 12$^{th}$ may, 2013 has been picked up by the pressure maps generated from OSCAT winds and are presented in figure 4. In-situ pressure observations were obtained from the moored buoy records available at Indian National Centre for Ocean Information Services (http://www.incois.gov.in) for validation. Nearly 77 collocated were available for comparison. The RMSD and bias are found to be $\pm$ 1.194 and + 0.028 respectively with $R^2$ value of 0.82.

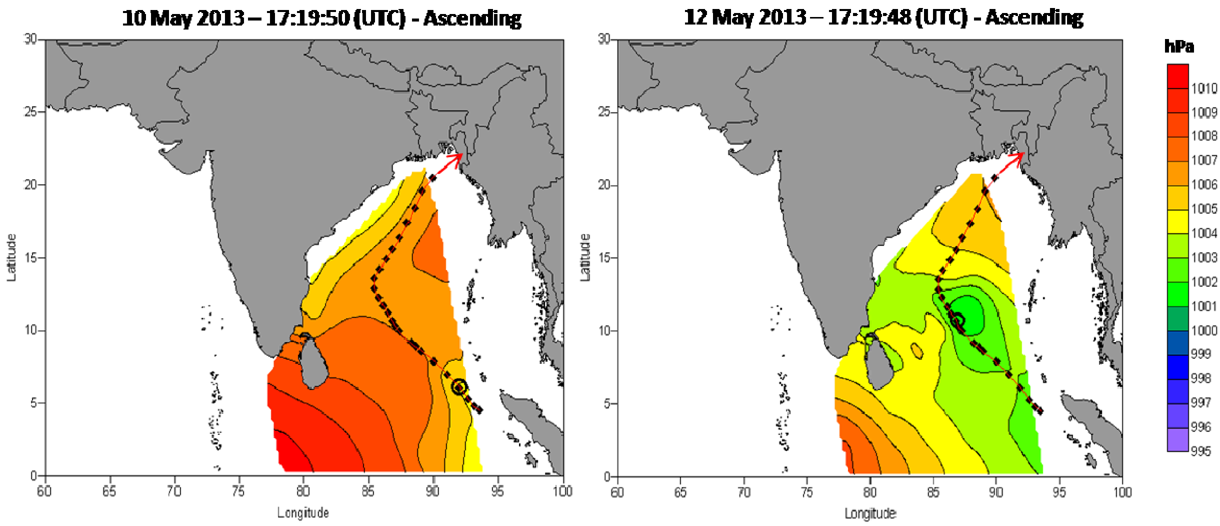


Figure 4. The image (left) is pressure fields derived from Oscat winds during the formation of Mahasen Cyclone, i.e. on 10$^{th}$ May, 2013, and the image (right) is the pressure fields during the Mahasen becoming severe cyclonic storm by 12$^{th}$ May, 2013.

## 5.4 Phailin

Cyclone Phailin is a tropical cyclone which emerged around 5 degrees east of Andaman and Nicobar islands on 7th Oct, 2013 and moved west-northwest. On the 8th of October, Phailin hit Andaman & Nicobar Islands and moved into the Bay of Bengal on the next day. Phailin rapidly intensified, and became a very severe cyclonic storm on October 10, equivalent to a category 1 hurricane on the Saffir-Simpson hurricane wind scale (SSHWS). Later that day, Phailin became equivalent to a category 4 hurricane on the SSHWS. The cyclone hit the Orissa and Andhra Pradesh coast on 12th Oct, 2013 (around 1600 hrs UTC). The information regarding Phailin cyclone obtained from India Meteorological Department (IMD, www.imd.gov.in). The cyclone prompted India's biggest evacuation in 23 years with more than 550,000 people moving up from the coastline in Odisha and Andhra Pradesh to safer places, 44 deaths have been reported during the cyclone.

The sea level pressure images retrieved from OSCAT winds using UWPBL model during Phailin Cyclone have been studied. It is seen from these images that pressure drop has been noticed 5-6 mb from 6th to 8th October, 2013 by 18:30 GMT (i.e. 24:00 IST, midnight of 8th) with closed isobars. As per IMD reports on 8th the Deep Depression upgraded to Cyclone and subsequently a cyclonic storm named it as Phailin. By nomenclature a pressure drop of 5 to 9 mb with maximum sustained 3 minutes surface winds of 34 knots or more is called as cyclonic storm, which is clearly observed in our satellite based pressure image/chart. It is further strengthened and formed into a very severe cyclonic storm by 10th and is clearly seen in the pressure image of that day. The closed isobars are highly depicted centered by less than 1000 mb (fig. 5). The Phailin is further intensified with a central pressure of 994 mb and crossed the coast near Gopalpur on 12th October, 2013 (fig. 6). These results are closely matching with IMD reports during this cyclone.

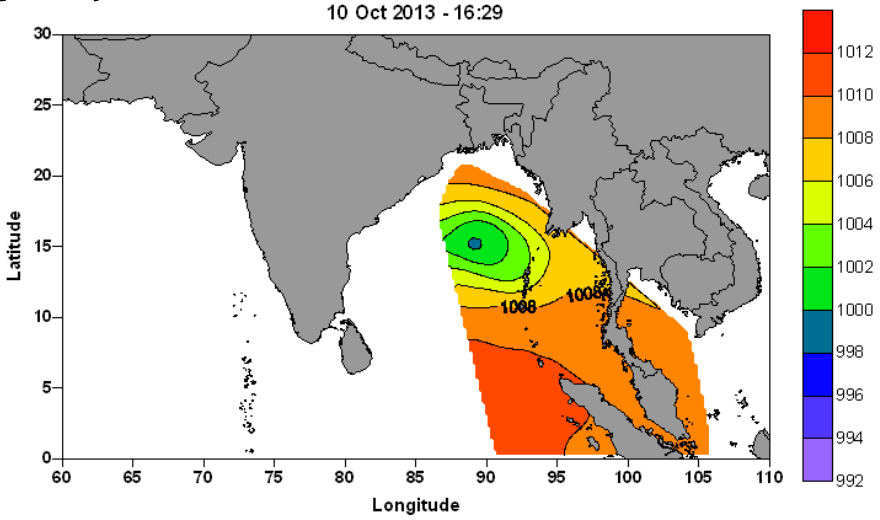


**Fig. 5.** Pressure fields retrieved from OSCAT winds using UWPBL model as on 10 October, 2013 at 16:29 GMT during Phailin cyclone with colour coded pressures in milli bars (mb) as background. Overlying with 2 mb interval isobars starting from 1000 mb to 1010 mb.

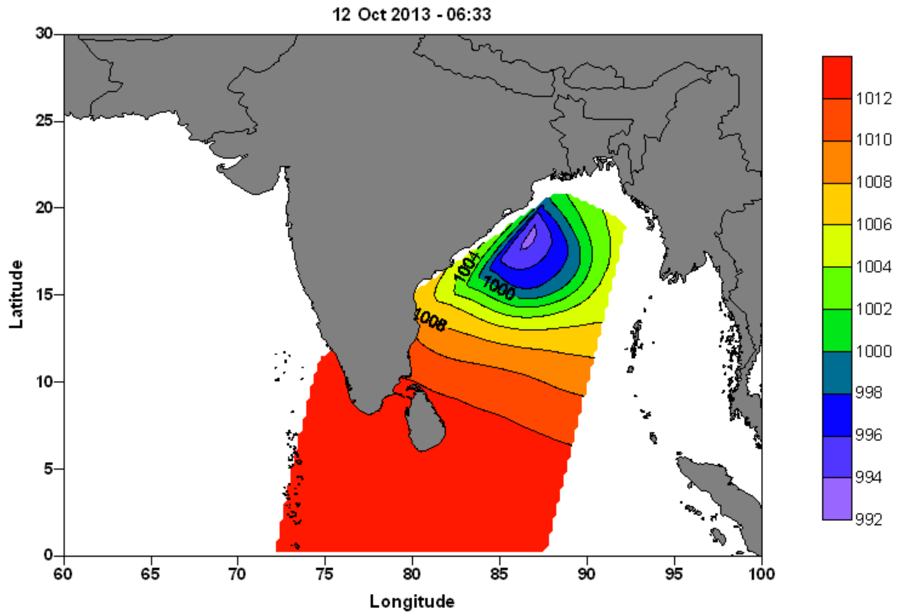


**Fig. 6.** Pressure fields retrieved from OSCAT winds using UWPBL model as on 12 October, 2013 at 06:33 GMT during Phailin cyclone with colour coded pressures in mb as background. Overlying with 2 mb interval isobars starting from 994 mb to 1012 mb.

### 5.5 Lehar

Lehar was the second most intense tropical cyclone of the 2013 season. It was named Lehar on November 24, after it had developed into a cyclonic storm. It gradually intensified further into a very severe cyclonic storm reaching its peak on November 26 with Hurricane winds of 140 km/h (87 mph) and a central pressure of 982 mbar (29.0 inHg) as reported by IMD, www.imd.gov.in. Thereafter, Lehar rapidly weakened into a depression and made landfall near Machilipatnam on November 28. It left lots of damage to the crops due to heavy rain fall during the cyclone.

During the cyclone Lehar, sea level pressure images from 21$^{st}$ to 28$^{th}$ November, 2013 have been generated using OSCAT winds. As per these images a demarcated low/Depression over Andaman Sea is observed on 23$^{rd}$ November, 2013. During mid day on 24$^{th}$ it was strengthened to a cyclonic storm and named as Lehar. By 25$^{th}$ evening it further intensified and turned into a severe cyclonic storm (fig. 7). It can be seen from the Pressure image (fig. 8) of 26$^{th}$ that the isobars are very closer and representing as Very Severe Cyclonic Storm. The cyclone Lehar has been weakened later and crossed the coast near Machilipatnam. The IMD report on the cyclone Lehar confirms these results.

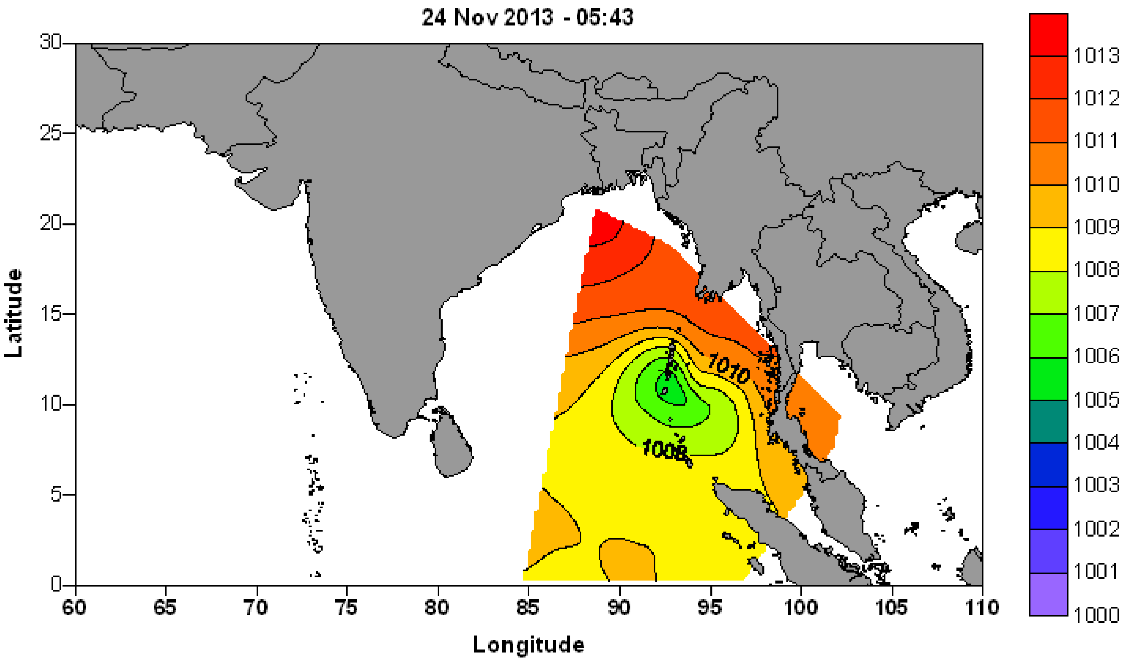


**Fig. 7**. Pressure fields retrieved from OSCAT winds using UWPBL model as on 24 November, 2013 at 05:43 GMT during Lehar cyclone with colour coded pressures in mb as background. Overlying with 1 mb interval isobars starting from 1006 mb to 1013 mb.

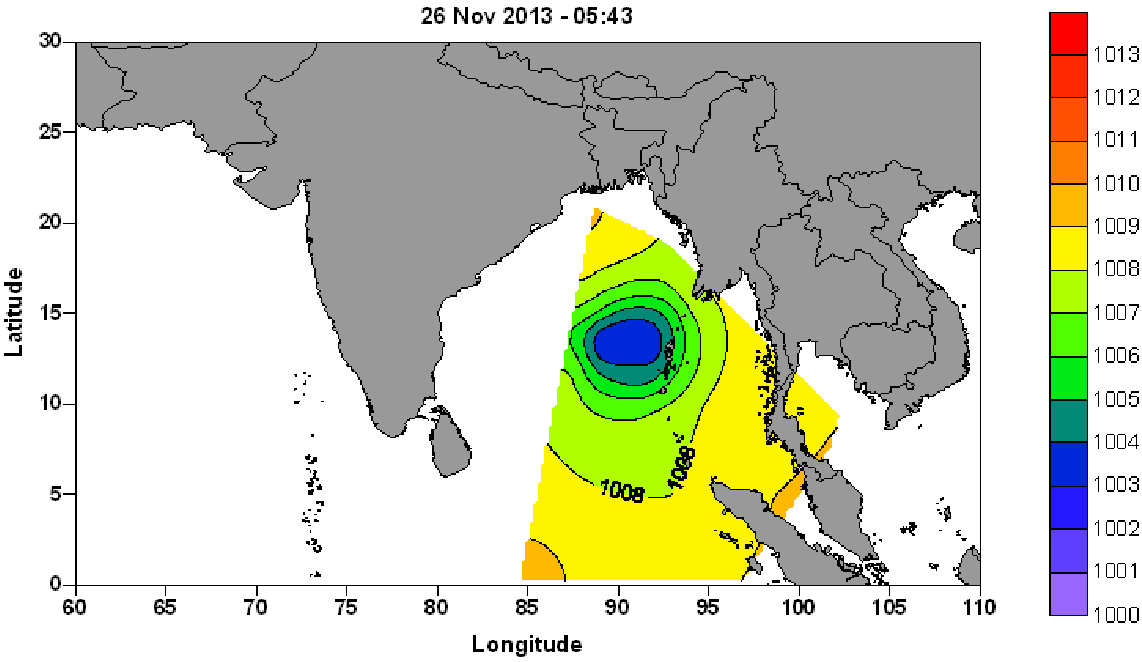


**Fig. 8**. Pressure fields retrieved from OSCAT winds using UWPBL model as on 26 November, 2013 at 05:43 GMT during Lehar cyclone with colour coded pressures in mb as background. Overlying with 1 mb interval isobars starting from 1004 mb to 1010 mb.

## 5.6 Madi

A low pressure area has been observed south of India close to the equator on November 30. The system slowly intensified in the next couple of days and IMD started tracking it and on early 07 December upgraded into a Deep Depression and later converted to cyclonic storm and named as Madi. By December 8, Madi had developed an excellent poleward outflow, with deep convection wrapped into a well-defined center with this, the IMD upgraded it to a Very Severe Cyclonic Storm, the third in 2013. IMD has reported winds of 65 knots (120 km/h; 75 mph) at the center. Overnight, Madi weakened further into a depression and crossed the Tamil Nadu coast close to Vedaranyam around 1330 UTC on December 12, 2013 left with highest rain fall of 115 mm in 24 Hrs.

Similarly we have used UWPBL model to generate sea level pressure images during Madi Cyclone also, from $6^{th}$ to $13^{th}$ December, 2013. The pressure images revealed that the formation of depression on $6^{th,}$ (fig. 9) intensification to very severe cyclonic storm by $8^{th}$ midnight/$9^{th}$ early morning (fig. 10) and it is weakened from next day onwards. The sequence of the events as observed from pressure images have fairly matched well with reports from IMD.

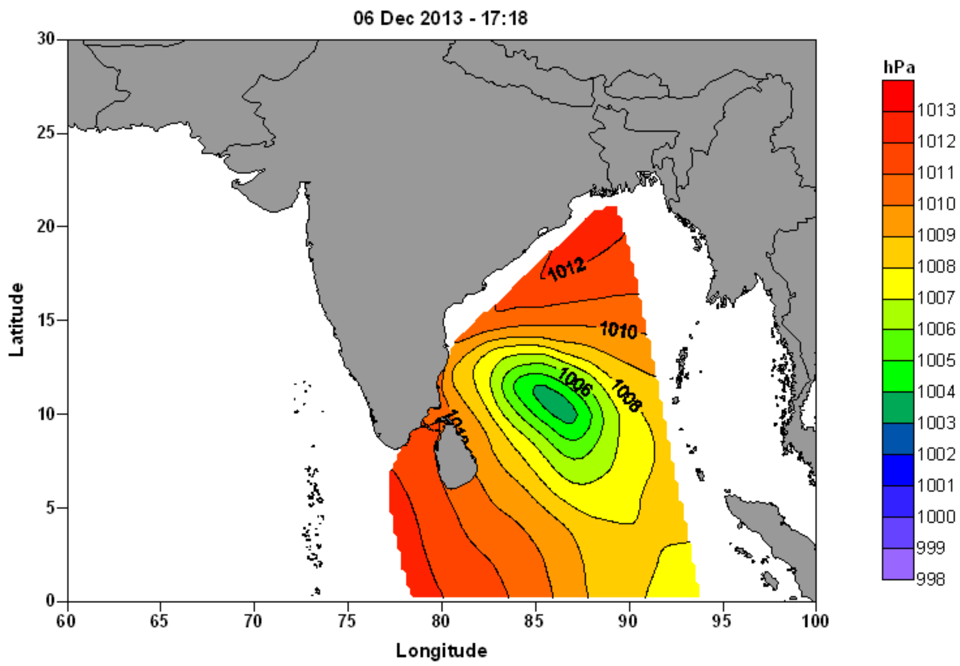


**Fig. 9.** Pressure fields retrieved from OSCAT winds using UWPBL model as on 06 December, 2013 at 17:18 GMT during Madi cyclone with colour coded pressures in mb as background. Overlying with 1 mb interval isobars starting from 1004 mb to 1012 mb.

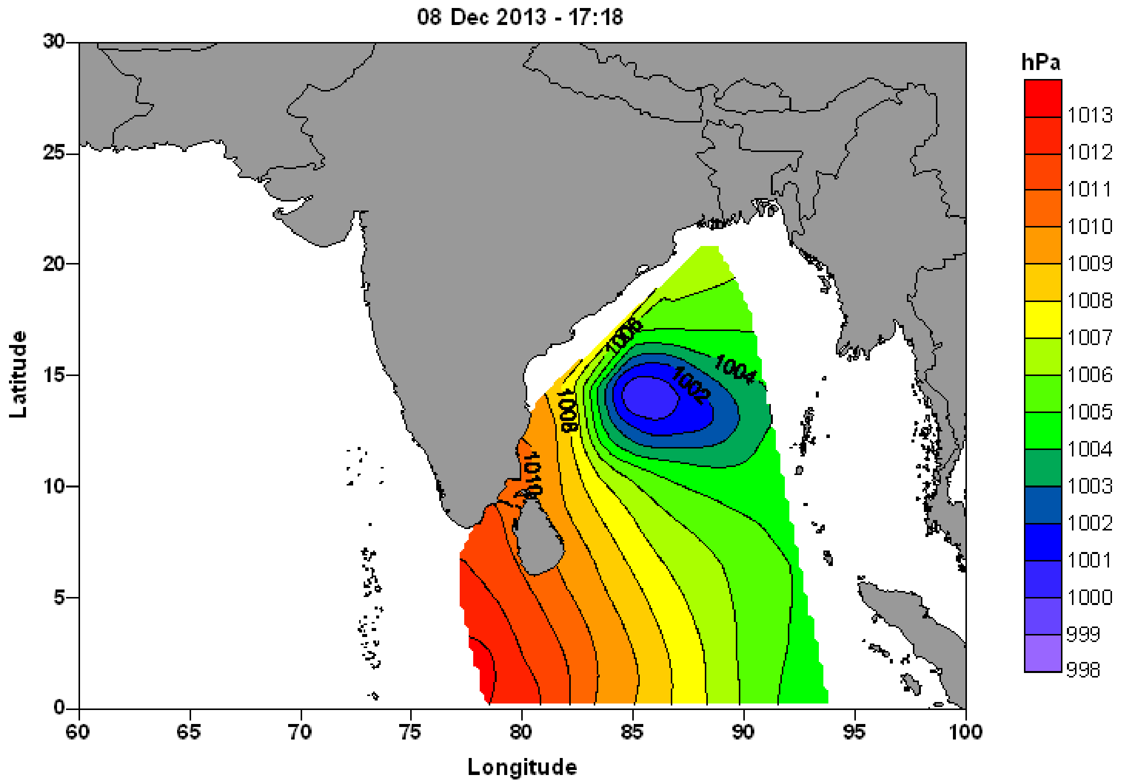


**Fig. 10.** Pressure fields retrieved from OSCAT winds using UWPBL model as on 08 December, 2013 at 17:18 GMT during Madi cyclone with colour coded pressures in mb as background. Overlying with 1 mb interval isobars starting from 1001 mb to 1014 mb.

## 5.7 Processing of QSCAT data

In addition, QSCAT Level 2B obtained from PO-DAAC site were also processes to retrieve the pressure fields retrieved during cyclone period in selected days in the years of 2004, 2005, 2007, 2008, 2009 over North Indian Ocean (NIO). The dates during cyclone period are selected from the cyclone bulletins and reports provided by IMD. In this period pressure fields generated with standard pressure as a first guess value and later the in-situ (Buoy) pressure observation averaged value as a first guess value to replace the standard pressure. The results are presented in this report.

In this study initially retrieved pressure fields over NIO using QSCAT wind data. Using this QSCAT wind ($0.25^0$ x $0.25^0$) data we generated the surface pressure fields ($0.5^0$ x $0.5^0$) over NIO on daily basis (pass wise) by given first guess value is a standard pressure value (1013 mb). After this study we considered some disturbances periods like cyclonic conditions and depressions periods. This information considered from Indian Meteorological Department (IMD) bulletins and reports.

## Retrieval & Validation of Pressure Fields from Scatterometer Winds

In this disturbance or cyclonic period times retrieved the pressure fields with standard pressure value as a first guess value and next in-situ pressure observations average value as a first guess value. We generated the pressure fields from the QSCAT winds in the normal condition (non-cyclonic or non-disturbance) days continuously for 3 months from Jan-Mar 2009 (178 Data sets), sample images of one day single pass of each month of January, February and March represented in figure 11.

Validation in the Normal day condition mentioned above period done with the in-situ (Moored Buoy) pressure observations. Co-located 308 points with the Buoy pressure observation with derived surface pressure field data. In this case the bias is **-0.05608 mb**, and the Root Mean Square Deviation (RMSD) is **± 1.655 mb**.

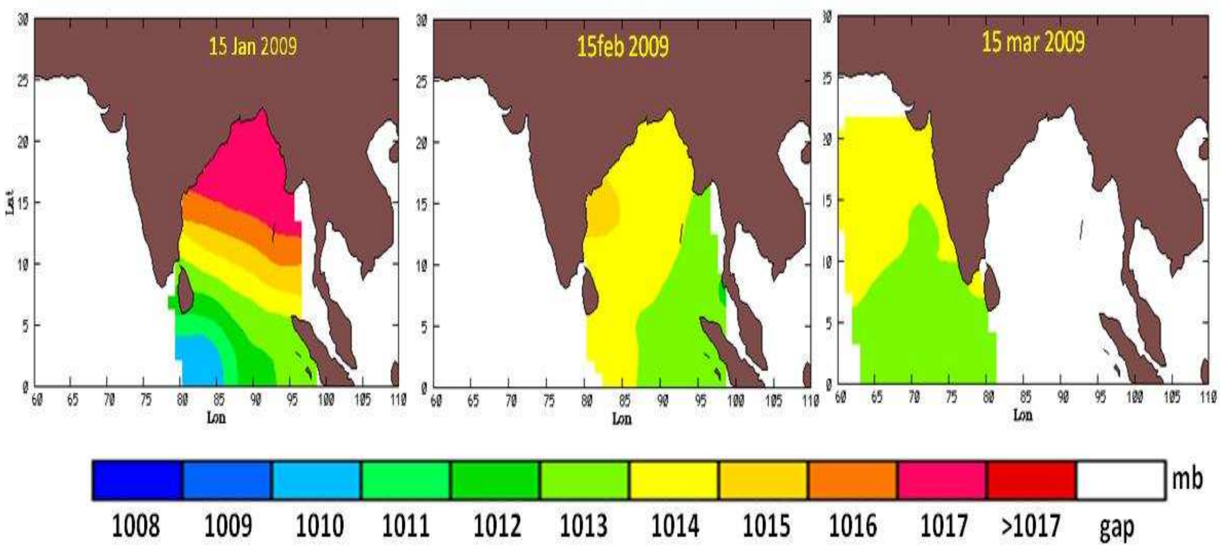


Figure 11. Images depicting the retrieved pressure fields during daily single pass of each month of January, February and March, 2009.

As well as pressure fields retrieved during cyclonic condition period in selected days in the years of 2004, 2005, 2007, 2008, 2009 over NIO and are presented in Table 1.

| Year | Month | Date |
|---|---|---|
| 2004 | May | 7,19 |
| 2005 | June | 27 |
| | July | 2,30 |
| | September | 15,16,17,18 |
| | October | 26 |
| | November | 30 |
| | December | 8,18 |
| 2007 | November | 11 |

| Year | Month | Date |
|---|---|---|
| 2008 | April | 30 |
| | November | 12,16,17 |
| 2009 | January | 15 |
| | April | 14,15,16,17 |
| | May | 23,24,25,26 |
| | November | 4,5,6,8,9,10 |

This date's taken from the cyclone bulletins and reports provided by IMD. In this period pressure fields generated with standard pressure value as a first guess value and in-situ (Buoy) pressure observation averaged value as a first guess value. Here buoy pressure observations where coming in the satellite path only considering, every pass collected buoy pressure observations and in that path time how many Buoy's pressure observations available that observations average value giving as a first guess value instead of standard pressure value. The validation of these days shown in the figure 12 and figure 13 this conditions Bias is **4.90575 mb** and RMSD is **± 5.7884 mb** with standard pressure (1013) as a first guess value. Bias is **-0.9726 mb** and RMSD is **± 2.2271 mb**. are Here co-located points are 89.

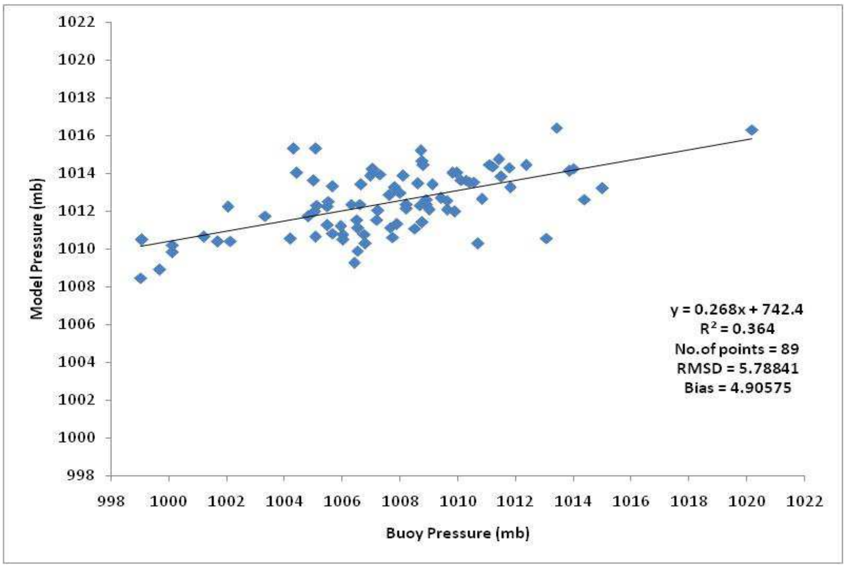


Figure 12 standard pressure value (1013 mb) is a first guess value.

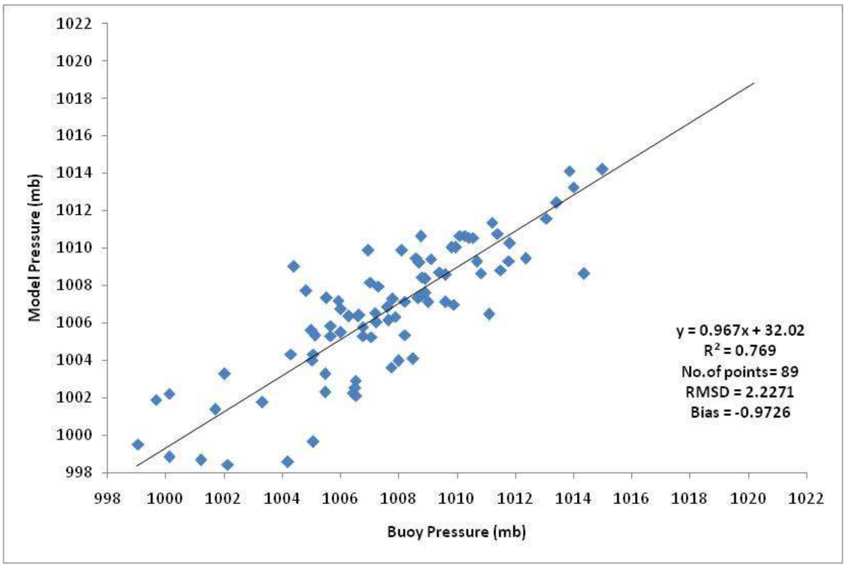


Figure 13 Buoy averaged pressure value is a first guess value.

In the year of 2009, three cyclones observed in April, May and November. Cyclone Bijili from 14th to 17th April, Cyclone Aila from 23rd to 26th May, Cyclone Phyan from 04th to 11th November 2009. In this periods also pressure fields retrieved using QSCAT winds. These three cyclone periods validation shown in the figure 14 and 15 this conditions Bias is **5.7185 mb** and RMSD is **± 6.3066 mb** with standard pressure (1013) as a first guess value. Bias is **-1.0814 mb** and RMSD is **± 2.05426 mb.** Here co-located points are 35.

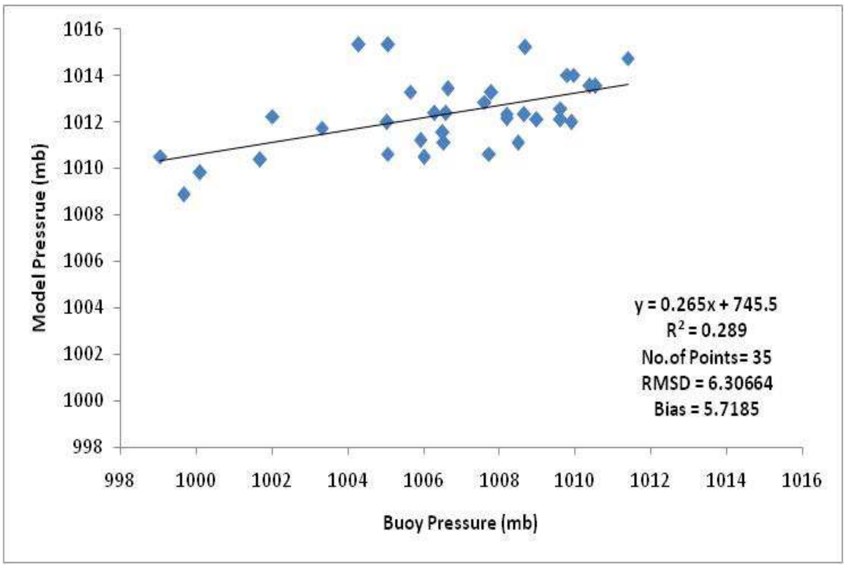


Figure 14. Standard pressure value (1013 mb) is a first guess value.

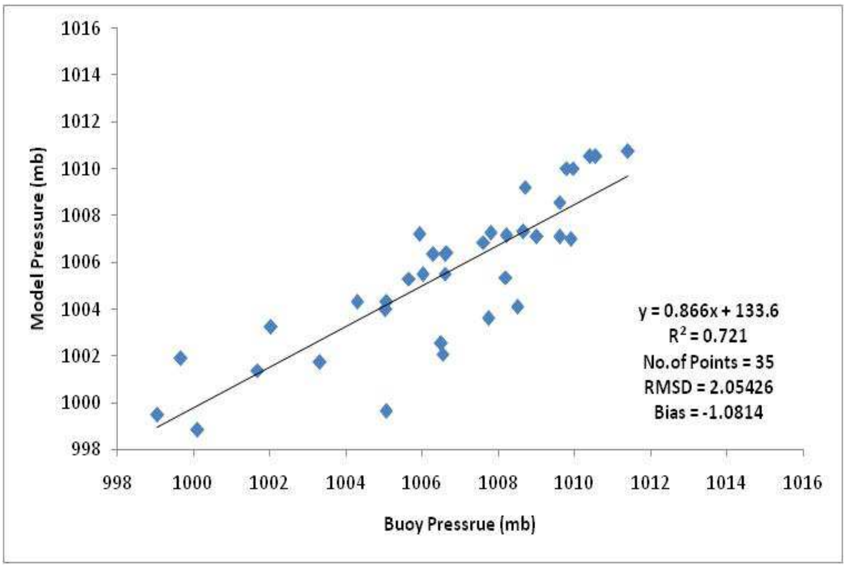


Figure 15. Buoy averaged pressure value is a first guess value.

### 6.0 Generation of global pressure field from OSCAT winds

The scatterometer onboard Oceansat-2 wind along track level-2B (non-gridded, 50 Km X50 Km) data is available from NRSC website in HDF (.h5) file format both ascending and descending. The wind data will be covered in 14 passes in a day. All the 14 passes are processed simultaneously to retrieve pressure fields with 2.5 deg. grid ECMWF pressure fields are given as first guess values to the UWPBL model. Then the individual passes are merged using *Data-Interpolating Variational Analysis (DIVA)* technique to generate global daily pressure fields from OSCAT winds. One of such product generated is presented in figure 16. Figure depicts very low pressure system in the northern Pacific Ocean and high pressure systems in the northern Atlantic Ocean, South Indian Ocean and also near Hawaii Islands in the Pacific. These trends are in line with Semi-permanent pressure systems during January.

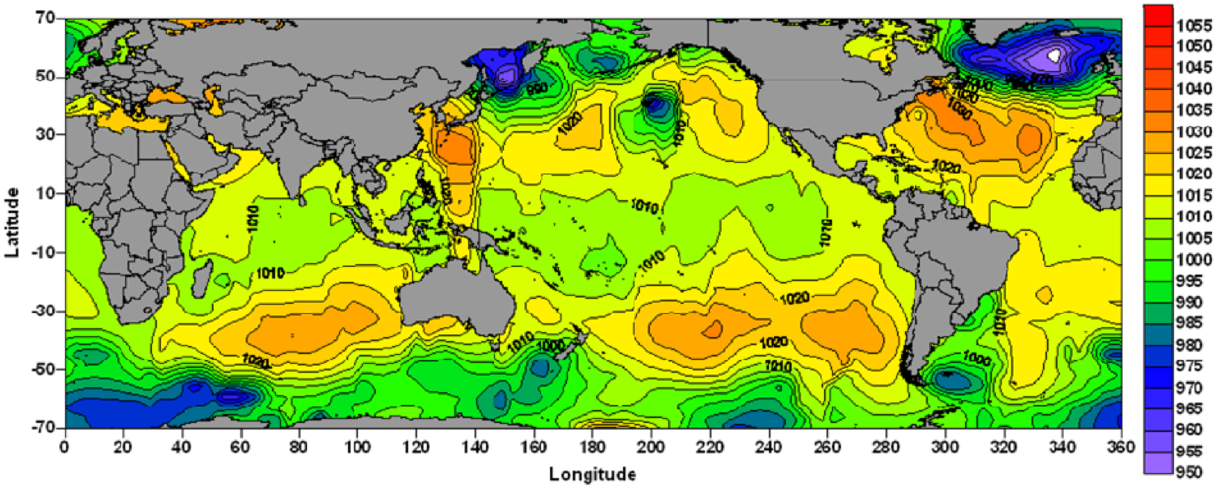


Figure 16. Sea Level Pressure fields from OSCAT winds on 19th January, 2011 (ECMWF 2.5 deg. grid SLP as first guess), covering the total globe overlying with 5 mb interval.

The validation exercise of the global products during January 2011 has been carried out using Drifting Buoys from GTS Provided by Fisheries and Oceans Canada. There are 19368 buoy observation are collected and co-located data set with satellite retrieved pressure fields were generated. The $R^2$ was found to be very good (0.84) and the scatter diagram of the same is presented in figure 17(A). To remove the out layers we have eliminated the data points fall outside the 3 sigma and the $R^2$ improved marginally (0.87) and the scatter diagram of the same is presented in figure 17(B). In addition we have collected moored buoy data from INCOIS during the same period (January, 2011) and number of observation are 19734 (both put together). The $R^2$ remains same (0.84) and the scatter diagram of the same is presented in figure 17(C).

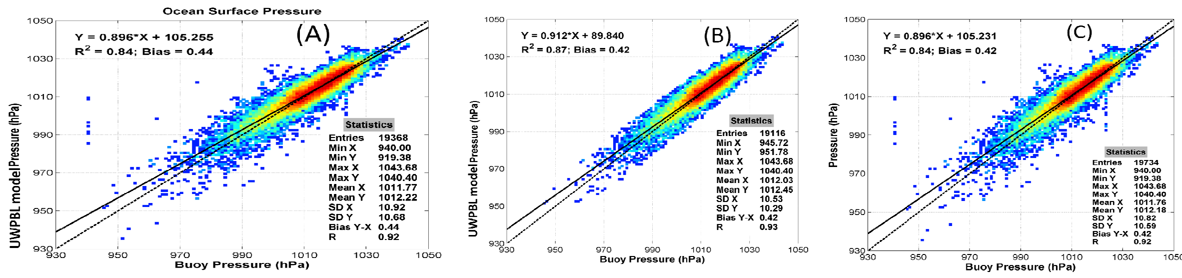


Figure 17 (A) Validation With Drifting Buoys from GTS Provided by Fisheries and Oceans Canada (B) Validation With Drifting Buoys from GTS Provided by Fisheries and Oceans Canada after considering the observation falling between ± 3 sigma (SD) and (C) Validation With Drifting Buoys from GTS Provided by Fisheries and Oceans Canada and Moored Buoys from INCOIS India.

### 7.0 Results

The UWPBL model initially implemented using Sea winds onboard Quik Scatterometer satellite winds to compute the pressure fields. Later the methodology has been extended using OSCAT winds.

We compare the intensity of the six very severe cyclonic storms based on the pressure images generated, it is observed that phailin cyclone found to be more severe compared to other five storms with a central pressure as low as 994 mb. However, the estimated central pressure reported by IMD during the peak of the storm is much less than this value, but patterns of isobars during all the storms are matching well with the reports available from other sources (IMD, JTWC). The errors in pressure values at the landfall are due to non availability of data points near shore.

The estimated sea-level pressure fields from OSCAT wind measurements using the University of Washington Planetary Boundary Layer (UWPBL) model. We compared the resulting sea-level pressure values with buoy (both mooring and drifting) measurements. Best results were obtained when all individual buoy measurements/course NWP model derivatives were taken as first guess pressure values to get actual pressure values from pressure gradients with low RMSD and high $R^2$ value. The bias is very small indicates the high accuracy of the estimations. The agreement between the scatterometer-derived sea level pressure field and the track information during cyclone speaks to the accuracy of both in track and intensity and usefulness of the model.

## 8.0 Conclusion

The estimated sea-level pressure fields are found to be useful in location, track and intensity of cyclone. In-situ measurements are closer to pressure estimated from scatterometer winds.

## 9.0 References

Brown, R. A., 1970: A secondary flow model for the planetary boundary layer. *J. Atmos. Sci.,* **27,** 742–757.

Brown, R. A., 1981: Modeling the geostrophic drag coefficient for AIDJEX. *J. Geophys. Res.,* **86,** 1989–1994

Brown R. A. and W. Timothy Liu, (1982): An Operational Large-Scale Marine Planetary Boundary Layer Model. *J. Appl. Meteor.*, **21**, 261–269.

Brown, R. A., (1998) Global high wind deficiency in modeling. *Remote Sensing of the Pacific Ocean by Satellites,* R. A. Brown, Ed., South wood Press Pvt. Limited, 69–77.

Brown, R. A., (2000) On satellite scatterometer model functions. *Journal of Geophysical Research,* **105,** 29 195–29 205.

Brown, R. A., and Levy G., (1986) Ocean surface pressure fields from satellite sensed winds. *Monthly Weather Review,* **114,** 2197–2206.

Brown, R. A., and Zeng L., (1994) Estimating central pressures of oceanic midlatitude cyclones. *Journal of Applied Meteorology,* **33,** 1088–1095.

Conaty, A. L., Jusem J. C., Takacs L., Keyser D., and Atlas R., (2001) The structure and evolution of extratropical cyclones, fronts, jet streams, and the tropopause in the GEOS general circulation model. *Bulletin of American Meteorological Society,* **82,** 1853–1867.

Foster, R. C., and Brown R. A., (1994) On large-scale PBL modelling: Surface wind and latent heat flux comparisons. *Global Atmospere-Ocean Systems,* **2,** 199–219.

Foster R C. and Gad Levy, 1998: The Contribution of Organized Roll Vortices to the Surface Wind Vector in Baroclinic Conditions. *J. Atmos. Sci.*, **55**, 1466–1472.

Foster, R. C., R. A. Brown, and A. Enloe, 1999: Baroclinic modifications of midlatitude marine surface wind vectors observed by the NASA scatterometer. *J. Geophys. Res.,* **104:**D24**,** 31 225–31 237.

Harlan, J., Jr. and O'Brien J. J., (1986) Assimilation of scatterometer winds into surface pressure fields using a variational method. *Journal of Geophysical Research,* **91,** 7816–7836.

Hsu, C. S., Wurtele M. G., Cunningham G. F., and Woiceshyn P. M., (1997) Construction of marine surface pressure fields from scatterometer winds alone. *Journal of Applied Meteorology,* **36,** 1249–1261.

Hsu, C. S., and Liu W. T., (1996) Wind and pressure fields near tropical cyclone Oliver derived from scatterometer observations. *Journal of Geophysical Research,* **101,** 17 021–17 027.

Levy, G., and Brown R. A., (1991) Southern Hemisphere synoptic weather from a satellite scatterometer. *Monthly Weather Review,* **119,** 2803–2813.

Patoux, J., (2000) UWPBL 3.0, The University of Washington Planetary Boundary Layer (UWPBL) Model. Techinical Note, University of Washington, 54 pp.

Patoux, J., and Brown R. A., (2001) A scheme for improving scatterometer surface wind fields. *Journal of Geophysical Research,* **106,** 23 985–23 994.

Patoux, J., and Brown R. A., (2002) A gradient wind correction for surface pressure fields retrieved from scatterometer winds. *Journal of Applied Meteorology,* **41,** 133–143.

Patoux, J., Foster R. C., and Brown R. A., (2003) Global Pressure Fields from Scatterometer Winds. *Journal of Applied Meteorology,* **42,** 813-826

Press, W. H., S. A. Teukolsky, W. T. Vetterling, and B. P. Flannery, 1992: *Numerical Recipes in FORTRAN: The Art of Scientific Computing.* Cambridge University Press, 963 pp.

Purna Chand Ch, M.V. Rao, I.V.Ramana, M.M.Ali, J Patoux, M.A.Bourassa (2014) Estimation of Sea-Level Pressure Fields during Cyclone Nilam from Oceansat-2 Scatterometer Winds. Atmos. Sci. Let. **15:** 65-71.

Report on Cyclonic Disturbances over North Indian Ocean during, 2005, 2007 and 2008, Pub: Regional Specialised Meteorological Centre-Tropical Cyclones, India Meteorological Department, New Delhi.

Stevens, B., Duan J., McWilliams J. C., Mu¨nnich M., and Neelin J. D., (2002) Entrainment, Rayleigh friction, and boundary layer winds over the tropical Pacific. *Journal of Climate,* **15,** 30–44.

Zeng, L., and Brown R. A., (1998) Scatterometer observations at high wind speeds. *Journal of Applied Meteorology,* **37,** 1412–1420.

Zeng, L., and Brown R. A., (2001) Comparison of planetary boundary layer model winds with dropwindsonde observations in tropical cyclones. *Journal of Applied Meteorology,* **40,** 1718–1723.

Zierden, D. F., Bourassa M. A., and O'Brien J. J., (2000) Cyclone surface pressure fields and frontogenesis from NASA scatterometer (NSCAT) winds. *Journal of Geophysical Research,* **105,** 23 967–23 981.

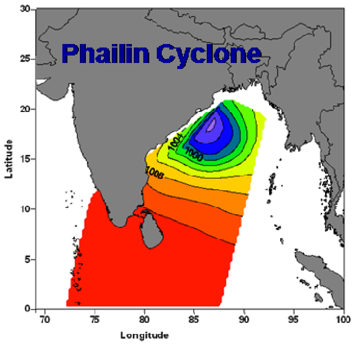


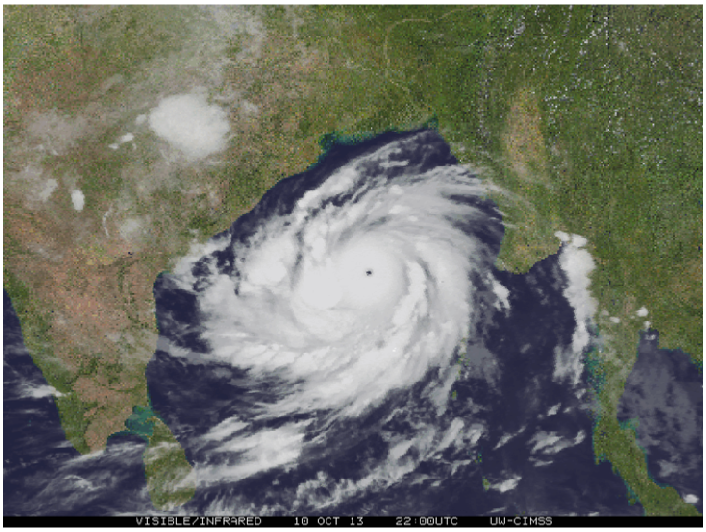


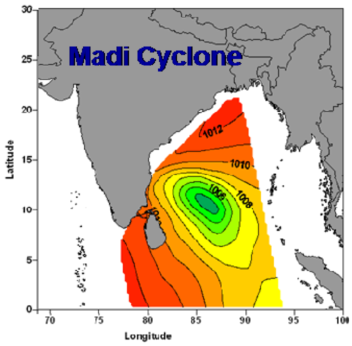


Ocean Sciences Group
(Earth and Climate Science Area)
National Remote Sensing Centre
ISRO (Govt. of India, Dept. of Space
Hyderabad, India

NRSC – ECSA – OSG – NOV - 2014 –TR - 667